PROCEEDINGS OF SPIE

SPIEDigitalLibrary.org/conference-proceedings-of-spie

Identifying and correcting pixel locking errors with the SPIFF algorithm

Yuval Yifat, Nishant Sule, Norbert F. Scherer

Yuval Yifat, Nishant Sule, Norbert F. Scherer, "Identifying and correcting pixel locking errors with the SPIFF algorithm," Proc. SPIE 10500, Single Molecule Spectroscopy and Superresolution Imaging XI, 105000N (20 February 2018); doi: 10.1117/12.2291267

SPIE.

Event: SPIE BiOS, 2018, San Francisco, California, United States

Downloaded From: https://www.spiedigitallibrary.org/conference-proceedings-of-spie on 3/7/2018 Terms of Use: https://www.spiedigitallibrary.org/terms-of-use

Identifying and correcting pixel locking errors with the SPIFF algorithm

Yuval Yifat[1,*], Nishant Sule[1], Norbert F. Scherer[1,2,*]
[1]James Franck Institute, The University of Chicago, IL 60637 USA; [2]Department of Chemistry, The University of Chicago, IL 60637 USA

ABSTRACT

Particle tracking is an important tool in a wide range of experimental fields in which optical imaging systems are used. Unfortunately, tracking algorithms are susceptible to pixel-locking when a tracked object occupies a small number of pixels on the detector or is near other particles, in which the particle localization is biased towards the pixel center. In this proceedings paper we demonstrate this effect and show how these errors can be ameliorated using the Single Pixel Interior Fill Function (SPIFF) algorithm, improving the fidelity of any metrics obtained from particle tracking (e.g interparticle separation). We analyze the severity of pixel bias inherent in optical systems of different magnification values and the effect that the SPIFF algorithm has on them. Our analysis demonstrates a tradeoff between the severity of the pixel locking and the signal-to-noise ratio of optical systems with different magnification.

Keywords: Optical trapping, microscopy, particle tracking, particle localization, algorithms.

1. INTRODUCTION

Imaging is a ubiquitous tool in scientific research, and as the capabilities of imaging systems and techniques improve, they allow one to observe increasingly smaller objects with greater frame rates and increased resolution[1], [2]. This has allowed remarkable scientific breakthroughs in a wide range of fields[3], [4]. Alongside the developments in imaging techniques there has been rapid development of algorithms for localizing and tracking objects in captured images. The input of these algorithms is a sequence of images, two-dimensional arrays of pixel intensities, and their output is determination of the pixel positions of bright (or dark) objects in the array – the localized coordinates of particles in the image. Such algorithms (e.g the Crocker-Grier algorithm[5]; the Raghuveer radial intensity algorithm[6]; non-linear fitting algorithms[7]) are exceedingly useful as they allow sub-pixel accuracy in determining the location of sub-micron scale objects and in extricating their dynamics and interactions in biological[8] and physical[9] systems.

However, when the tracked objects are small (occupy a small number of pixels on the detector), or are in close proximity to other objects most tracking algorithms introduce pixel-locking error, in which the particle localization is biased towards the center of the pixel (see Fig 1). As a result, any metric obtained from the tracked particle trajectory such as mean square displacement[10] (MSD) or interparticle separation will also be biased and inaccurate.

Fortunately, Burov et al[11] introduced the Single Pixel Interior Fill Function (SPIFF) algorithm that corrects pixel-locking errors. The SPIFF algorithm is highly useful at reducing errors in the fidelity of the tracked particle trajectories, and in metrics such as interparticle separation or orientation[12].

In this proceedings paper, we analyze the effect that different microscope magnification values have on the severity of pixel locking and on the efficacy of the SPIFF algorithm. We captured videos of a single 150 nm Ag nanoparticle trapped in a focused Gaussian optical beam. The particle was imaged using different optical magnification values (60x, 90x, 150x and 225x). We applied standard particle tracking methods[13] to localize the particle positions and compared the severity of pixel locking observed for each of the magnification values. We then applied the SPIFF algorithm to the tracked trajectories and compared the output for the different magnifications. We report a tradeoff between the pixel-locking we observe for smaller magnification values and the signal-to-noise ratio (SNR) of the captured image seen in larger magnifications.

*Corresponding authors: yuvalyifat@uchicago.edu; nfschere@uchicago.edu

Single Molecule Spectroscopy and Superresolution Imaging XI, edited by Jörg Enderlein, Ingo Gregor, Zygmunt Karol Gryczynski, Rainer Erdmann, Felix Koberling, Proc. of SPIE Vol. 10500, 105000N
© 2018 SPIE · CCC code: 1605-7422/18/$18 · doi: 10.1117/12.2291267

Downloaded From: https://www.spiedigitallibrary.org/conference-proceedings-of-spie on 3/7/2018 Terms of Use: https://www.spiedigitallibrary.org/terms-of-use

2. PIXEL LOCKING AND THE SPIFF ALGORITHM

2.1 Pixel locking

Commonly used particle tracking algorithms[6], [13], [14] make use of a circular fitting window with a width of $W=2R+1$ pixels as their basis for identifying and localizing particles in an image. By fitting of the tracking window to the 2D array of pixel intensities in a given frame the output of the algorithms is a table of calculated particle positions $\{x_n,y_n\}$. In cases when the imaged objects are small (i.e. 2-4 pixels FWHM on the detector), and close together (e.g. 2-5 pixels separation on the detector) the tracking has to be done using the algorithm's smallest possible window size for particle identification and Gaussian fitting or centroid localization. However, such a small window size is susceptible to a Nyquist undersampling error that results in a systematic error known as pixel locking[15] in which the particle positions are biased towards the center of the pixel.

This error can be seen in Figure 1, which shows a representative frame from a video of three 150 nm Ag nanoparticles tracked with a window size of $R=1,2$ and 3 (Fig 1a-c). These frames were taken from a 1000 frame video. We tracked the entire video using the aforementioned window sizes and collected a set of the decimal parts of the localized positions as a 2D distribution. Each of these distributions shown in Fig 1(d-f) is termed a "meta-pixel". These distributions show the particle positions are severely biased towards the center of the pixel (blue points are individual localizations) fir small tracking window sizes introducing a localization error that (strongly) effects the calculation of metrics such as interparticle separation and orientation values.

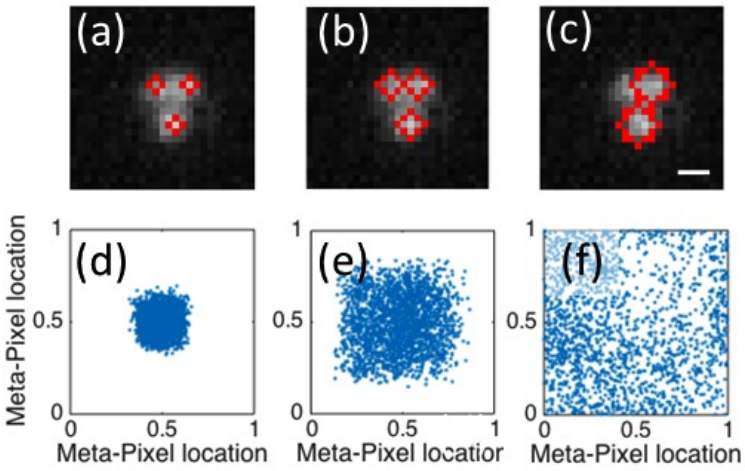

Figure 1. (a-c) Dark-field microscopy images of three 150nm Ag nanoparticles in a Gaussian optical trap. The red marks on the bright pixels are the results of localization using the Mosaic particle tracking algorithm suite from imageJ[13] with radius of $R=1,2$ and 3 pixels respectively (tracked particle diameter is $W=2R+1$). Scale bar is 350 nm. (b) Resultant decimal particle localizations, termed the "meta-pixel", calculated by tracking a 1000 frame video of three Ag nano-particles. Each frame represents the result of tracking the video using the tracking radii shown in (a)-(c).

A larger percentage of the particles can be identified, even when the particles are closely separated, when the tracking window is small (e.g. $R=1$), however, we observe a strong pixel-locking which introduces errors in position dependent metrics. Conversely, when a large tracking window is used (e.g. $R=3$), the pixel-locking bias disappears, but many particles are not identified (one of the three particles in figure 1(c) is not identified).

2.2 The SPIFF Algorithm

The pixel locking bias can be removed by using the Single Pixel Interior Filling Function (SPIFF) method, which is a corrective algorithm introduced by Burov et al[11]. The SPIFF algorithm collects the fractional part of the tracked locations in a meta-pixel. It proceeds to estimate the true particle position of a given particle localization by expanding the probability distribution such that it uniformly spans the entire meta-pixel. Given a set of estimated decimal values of the localized particle centers $\{\hat{X}_E\}$, the true particle position $\hat{X}_T$ can be calculated by numerically solving the integral

Downloaded From: https://www.spiedigitallibrary.org/conference-proceedings-of-spie on 3/7/2018 Terms of Use: https://www.spiedigitallibrary.org/terms-of-use

$$\hat{X}_T = \pm \int_0^{X_E} P(\hat{X}'_E) d\hat{X}'_E, \quad (1)$$

and finding the fraction of estimated values in the range $(0, \hat{X}_E)$, where $P(\hat{X}'_E)$ is the SPIFF density function, i.e. the probability density of the set $\{\hat{X}_E\}$. For more details see refs.[11], [12] Figure 2 shows an example of a meta-pixel distribution for a video of two particles in a Gaussian optical trap before and after application of the SPIFF correction algorithm. As can be seen from Figure 2, the SPIFF algorithm evenly distributes the particle localizations across the meta-pixel, leading to a more uniform distribution.

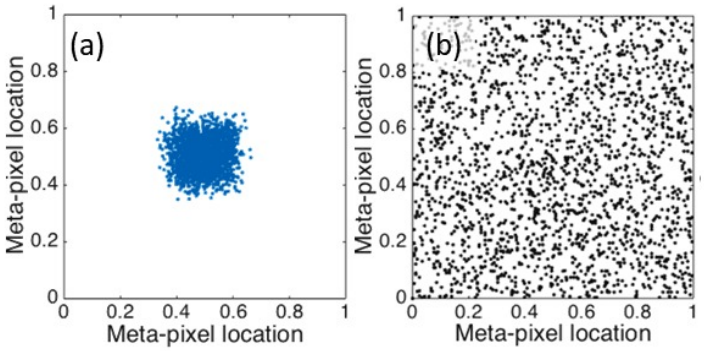

Figure 2. Decimal part of the pixel localization in a ”meta-pixel”. The localizations are from the tracked data of an experimental video of two particles in a optical Gaussian trap before (a; blue) and after (b; black) SPIFF correction. Data was taken from an experimental video with 1000 frames and 2000 particle localizations.

3. COMPARISON BETWEEN DIFFERENT MICROSCOPE MAGNIFICATIONS

As shown in Figure 1, choosing a small tracking window introduces greater bias in the particle localizations and larger pixel locking. In theory this effect could be counteracted by choosing an optical system with greater magnification. The magnification of the optical system directly determines the size of the particles on the detector (i.e. the number of in pixels it occupies on the detector) as it determines the effective pixel size of the system. Therefore, one might assume that increasing the magnification of the system would allow for a smaller effective pixel and a larger image of the particle, which in turn allows one to increase the size of the tracking window and to circumvent the issue of pixel locking.

However, increasing the magnification will decrease the SNR of the system, as the same number of photons will now be spread over a larger number of pixels, thereby affecting the precision of localization. This is of particular concern in the case of photon-limited experiments such as imaging of single fluorescent molecules or rapidly moving particles that necessitate short integration times.

In order to explore the effect of magnification on the SPIFF algorithm, we trapped a single 150nm diameter Ag nanoparticle in an expanded Gaussian trap using the setup described by Sule et al[16]. The particle motion was captured at a frame rate of 2004FPS with an exposure time of 100 μs and the videos were 10^4 frames long. These imaging conditions are commonly used in experiments set up to capture fast dynamics of trapped particles. We also introduced an external 2.5x beam expander to the system allowing us to capture the particle motion with magnifications of 60x, 90x, 150x and 225x, corresponding to effective pixel sizes of 108, 72, 43 and 29 nm, respectively. Figure 3 shows a representative frame from the videos taken for each of the magnifications.

Downloaded From: https://www.spiedigitallibrary.org/conference-proceedings-of-spie on 3/7/2018 Terms of Use: https://www.spiedigitallibrary.org/terms-of-use

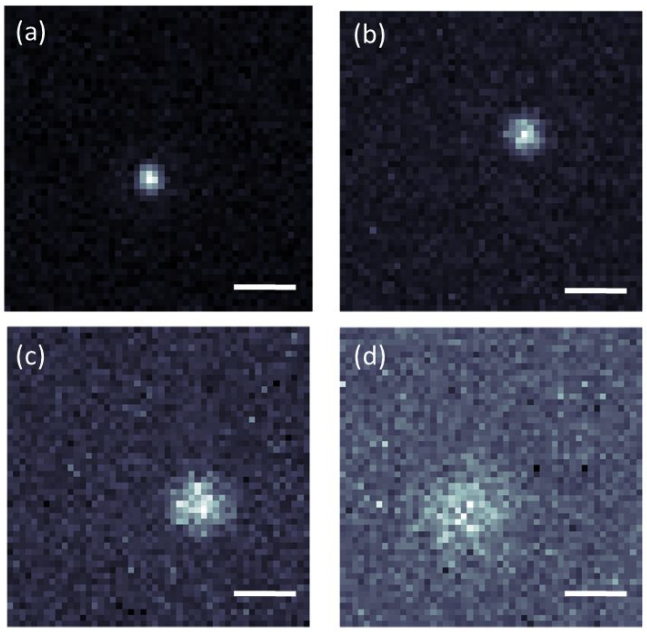

Figure 3. Representative dark-field image of a single 150 nm Ag nanoparticle taken at different magnifications. (a) 60x magnification, scale bar is 1080 nm. (b) 90x magnification, scale bar is 720 nm. (c) 150x magnification, scale bar is 430 nm. (d) 225x magnification, scale bar is 288 nm. The illumination intensity was the same for all magnifications

As can be seen from Fig 3, the size of the particle on the detector increases at larger magnifications, but its contrast is reduced (compared to the background). This is due to the fact that the light scattered from the particle is distributed amongst more pixels. We measured the SNR of the videos (defined as the ratio of the brightest pixel in the particles to the mean value of the background pixels) for the different magnifications as 3.3, 2.4, 1.7 and 1.4 for the aforementioned magnifications.

We tracked the particle positions using the Mosaic program with varying window radii and used the tracked trajectories to calculate the mean square displacement (MSD) values for the trapped particle. The MSD of a tracked particle is defined as:

$$MSD(\tau) = \overline{(\vec{x}(t+\tau) - \vec{x}(\tau))^2}\,, \qquad (2)$$

where $\vec{x}(\tau)$ is the position of a particle at time τ, and $\vec{x}(t+\tau)$ is its position after time t. The overbar in the equation signifies the mean of the displacement difference. MSD is an widely used measure that is used to determine the nature of particle motion in a wide range of fields such as biophysics[9] or colloidal systems[17]. This measure is often used to examine the statistical mechanical properties of diffusing and driven particles of interest.

Figure 4 compares the MSDs for a single particle trapped under identical trapping conditions but viewed under different magnifications. Thus, the physical behavior of the particle will be the same and any differences in the tracked particle behavior will be due to the differences in the magnification. Note that all the MSD vs. lag time plots are curved due to the particle feeling the limited (confined volume of the optical trap. When the magnification is small (see Fig. 4(a)), the accuracy of the particle localization is limited by pixel locking effects. As a result, the particle displacement at small time lags (the first step of the MSD) is larger than for the 90x magnification (Fig 4(b)). This error can be improved significantly by using the SPIFF algorithm (compare the dashed and solid curves in Fig 4a).

When the magnification is large (e.g. Fig 4d) we see that the SPIFF algorithm does not significantly improve the MSD, for any tracking window size. This is because the tracked data do not exhibit pixel-locking so the SPIFF algorithm has nothing to correct for larger windows (e.g. R=5 in panel (d)). For smaller windows (R=2 in panels (c-d)) the localization accuracy is limited by the low SNR of the images, which causes the tracking algorithm to have poor precision; that is, the particle position is localized to different pixels (from frame to frame) and thus localizations are not necessarily on its

Downloaded From: https://www.spiedigitallibrary.org/conference-proceedings-of-spie on 3/7/2018 Terms of Use: https://www.spiedigitallibrary.org/terms-of-use

true center. This imprecise localization results in artificially large displacements. These precision-limited effects are present in both the 150x (Fig 4(c)) and the 225x (Fig S(d)) magnifications.

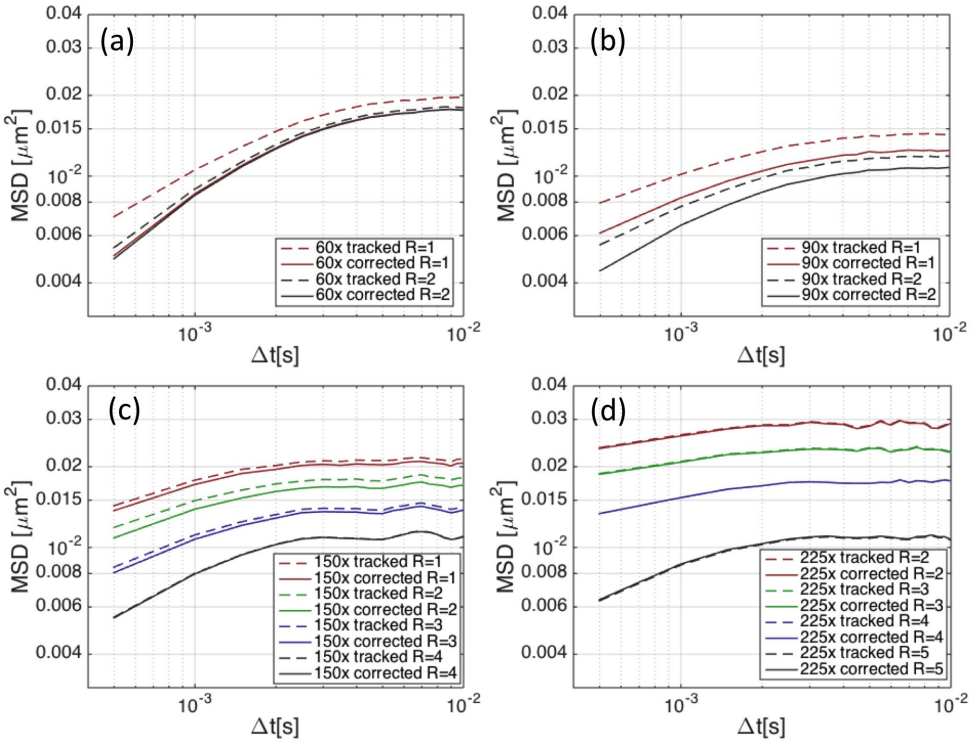

Figure 4. Calculated MSD values for a single particle trapped in a focused Gaussian trap for magnifications of (a) 60x, (b) 90x (c) 150x and (d) 225x. The different colored curves represent the different window sizes used by the Mosaic algorithm for particle tracking. The dashed curves are the tracked data, while the solid curves are the results calculated for the same trajectories after SPIFF correction. Note that the scale is the same for all calculations.

Figure 5 shows a comparison between the calculated MSD results for the largest tracking windows for all magnifications shown in Figure 4 (i.e. *R=2* for 60x and 90x magnifications, *R=4* for 150x magnification and *R=5* for 225x magnification). The curves in Figure 5 show the results obtained from the MSD calculations of each of the magnifications using the largest reasonable tracking window sizes (that is, window sizes that are not larger than the tracked particle). The 90x magnification data gives the smallest initial MSD value, implying that this magnification allows the best accuracy and precision in particle localization. This magnification is in accordance with the requirement that the pixel size be roughly 1/2.8 of the diffraction limit of the system[18]. It is important to note that this result is only valid for the optical system and trapping parameters described in section 1. A change in the noise of the system (obtainable by increasing the exposure time) or the particle brightness and size could lead to a different optimal magnification. For example, for brighter particles (and lower detector noise and background levels) greater magnification might be better. More research needs to be done to make a general claim about the optimal conditions for extracting information about sub-pixel particle positions given a system's SNR and the measured objects brightness and dimensions.

It is worth noting that the improvement of the MSD calculations by the SPIFF correction for the lowest magnification (evident in Figure 4(a) and in the red curves of Fig. 5) is a mark of the SPIFF algorithm restoring some of the information about the particle trajectory lost due to pixel-locking. Therefore, one could increase the sampling rate of a given experiment without much loss of information by using lower magnification and a smaller field of view, which would allow a higher frame rate, and applying the SPIFF correction to the resulting trajectories.

Downloaded From: https://www.spiedigitallibrary.org/conference-proceedings-of-spie on 3/7/2018 Terms of Use: https://www.spiedigitallibrary.org/terms-of-use

Regardless, since the experimental configuration we used is common amongst similar optical trapping and imaging experiments of plasmonic nanoparticles[19], [20] or Quantum dots[21], [22], we can claim that the optimal conditions we have found (a magnification of 90x combined with SPIFF correction of the tracked results) are applicable to a wide range of experimental results.

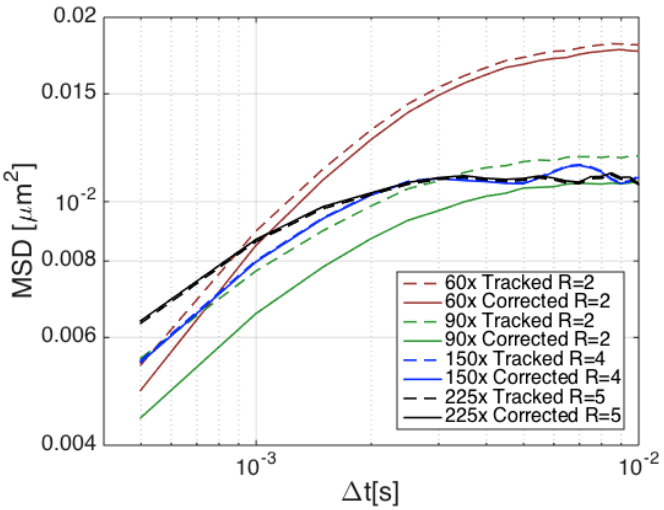

Figure 5. Comparison between the MSD values calculated from different magnification values. The results shown here were chosen as the larges possible tracking window that is not larger than the particles for each one of the magnification values.

4. CONCLUSIONS AND FUTURE WORK

We have discussed the pixel-locking bias that arises when trying to image small particles such as nano-particles or single fluorescent molecules, and the SPIFF algorithm that is used to correct this bias. We utilized a single optically trapped 150 nm Ag nanoparticle and tracked its position using commonplace particle tracking methods. Using the MSD of the particle, we demonstrated the tradeoff between the SNR of an image and pixel locking bias it presents (which necessitated the use of the SPIFF algorithm). Our results hints at a larger opportunity – since the SPIFF algorithm allows us to use smaller magnification and still capture the average physical characteristics of the system, it could be thought of as a compressed sensing mechanism.[23], [24] In future work we will focus on generalizing the conditions necessary for defining the optimal magnification for a given particle size and photon budget. This could be used to improve the resolution and acquisition rate of optical imaging and microscopy studies.

5. ACKNOWLEDGEMENTS

The authors acknowledge support from the Vannevar Bush Faculty Fellowship program sponsored by the Basic Research Office of the Assistant Secretary of Defense for Research and Engineering and funded by the Office of Naval Research through grant N00014-16-1-2502.

6. REFERENCES

[1] A. R. Small and R. Parthasarathy, “Superresolution Localization Methods,” *Annu. Rev. Phys. Chem.*, vol. 65, no. 1, pp. 107–125, 2014.

[2] K. I. Willig, S. O. Rizzoli, V. Westphal, R. Jahn, and S. W. Hell, “STED microscopy reveals that synaptotagmin remains clustered after synaptic vesicle exocytosis.,” *Nature*, vol. 440, no. 7086, pp. 935–939, Apr. 2006.

[3] M. K. Cheezum, W. F. Walker, and W. H. Guilford, “Quantitative Comparison of Algorithms for Tracking Single Fluorescent Particles,” *Biophys. J.*, vol. 81, no. 4, pp. 2378–2388, 2001.

[4] N. Chenouard, I. Smal, F. de Chaumont, M. Maška, I. F. Sbalzarini, Y. Gong, J. Cardinale, C. Carthel, S.

Downloaded From: https://www.spiedigitallibrary.org/conference-proceedings-of-spie on 3/7/2018 Terms of Use: https://www.spiedigitallibrary.org/terms-of-use

Coraluppi, M. Winter, A. R. Cohen, W. J. Godinez, K. Rohr, Y. Kalaidzidis, L. Liang, J. Duncan, H. Shen, Y. Xu, K. E. G. Magnusson, J. Jaldén, H. M. Blau, P. Paul-Gilloteaux, P. Roudot, C. Kervrann, F. Waharte, J.-Y. Tinevez, S. L. Shorte, J. Willemse, K. Celler, G. P. van Wezel, H.-W. Dan, Y.-S. Tsai, C. Ortiz de Solórzano, J.-C. Olivo-Marin, and E. Meijering, "Objective comparison of particle tracking methods.," *Nat. Methods*, vol. 11, no. 3, pp. 281–9, Mar. 2014.

[5] J. Crocker and D. G. Grier, "Methods of Digital Video Microscopy for Colloidal Studies," *J. Colloid Interface Sci.*, vol. 179, pp. 298–310, 1996.

[6] R. Parthasarathy, "Rapid, accurate particle tracking by calculation of radial symmetry centers," *Nat. Methods*, vol. 9, no. 7, pp. 724–726, Jun. 2012.

[7] X. Qu, D. Wu, L. Mets, and N. F. Scherer, "Nanometer-localized multiple single-molecule fluorescence microscopy.," *Proc. Natl. Acad. Sci. U. S. A.*, vol. 101, no. 31, pp. 11298–303, 2004.

[8] H. Jin, D. A. Heller, and M. S. Strano, "Single-particle tracking of endocytosis and exocytosis of single-walled carbon nanotubes in NIH-3T3 cells," *Nano Lett.*, vol. 8, no. 6, pp. 1577–1585, Jun. 2008.

[9] Y. Lin, T. Zhao, X. Jian, Z. Farooqui, X. Qu, C. He, A. R. Dinner, and N. F. Scherer, "Using the bias from flow to elucidate single DNA repair protein sliding and interactions with DNA," *Biophys. J.*, vol. 96, no. 5, pp. 1911–1917, 2009.

[10] E. Kepten, A. Weron, G. Sikora, K. Burnecki, and Y. Garini, "Guidelines for the fitting of anomalous diffusion mean square displacement graphs from single particle tracking experiments," *PLoS One*, vol. 10, no. 2, 2015.

[11] S. Burov, P. Figliozzi, B. Lin, S. A. Rice, N. F. Scherer, A. R. Dinner, J. Crocker, and E. R. Weeks, "Single-pixel interior filling function approach for detecting and correcting errors in particle tracking," *Proc. Natl. Acad. Sci.*, p. 201619104, 2016.

[12] Y. Yifat, N. Sule, Y. Lin, and N. F. Scherer, "Analysis and correction of errors in nanoscale particle tracking using the Single-pixel interior filling function (SPIFF) algorithm," *Scientific reports*, vol. 7, no. 1, p. 16553, Dec. 2017.

[13] I. F. Sbalzarini and P. Koumoutsakos, "Feature point tracking and trajectory analysis for video imaging in cell biology," *J. Struct. Biol.*, vol. 151, no. 2, pp. 182–195, 2005.

[14] S. S. Rogers, T. A. Waigh, X. Zhao, and J. R. Lu, "Precise particle tracking against a complicated background: polynomial fitting with Gaussian weight.," *Phys. Biol.*, vol. 4, no. 3, pp. 220–227, 2007.

[15] J. C. Crocker and B. D. Hoffman, "Multiple-Particle Tracking and Two-Point Microrheology in Cells," *Methods in Cell Biology*, vol. 83. pp. 141–178, 2007.

[16] N. Sule, Y. Yifat, S. K. Gray, and N. F. Scherer, "Rotation and Negative Torque in Electrodynamically Bound Nanoparticle Dimers," *Nano Lett.*, vol. 17, no. 11, p. acs.nanolett.7b02196, Sep. 2017.

[17] X. Zheng, B. Ten Hagen, A. Kaiser, M. Wu, H. Cui, Z. Silber-Li, and H. Löwen, "Non-Gaussian statistics for the motion of self-propelled Janus particles: Experiment versus theory," *Phys. Rev. E - Stat. Nonlinear, Soft Matter Phys.*, vol. 88, no. 3, 2013.

[18] J. B. Pawley, "Fundamental limits in confocal microscopy," in *Handbook of biological confocal microscopy*, 3rd ed., Springer, 2006, pp. 59–79.

[19] P. Figliozzi, N. Sule, Z. Yan, Y. Bao, S. Burov, S. K. Gray, S. A. Rice, S. Vaikuntanathan, and N. F. Scherer, "Driven optical matter: Dynamics of electrodynamically coupled nanoparticles in an optical ring vortex," *Phys. Rev. E*, vol. 95, no. 2, p. 22604, 2017.

[20] M. Siler and P. Zemanek, "Particle jumps between optical traps in a one-dimensional (1D) optical lattice," *New J. Phys.*, vol. 12, no. 8, p. 83001, Aug. 2010.

[21] Z. Yan, U. Manna, W. Qin, A. Camire, P. Guyot-Sionnest, and N. F. Scherer, "Hierarchical Photonic Synthesis of Hybrid Nanoparticle Assemblies."

[22] Y. Yifat, M. Ackerman, and P. Guyot-Sionnest, "Mid-IR colloidal quantum dot detectors enhanced by optical nano-antennas," *Cit. Appl. Phys. Lett*, vol. 110, no. 101, 2017.

[23] G. Kutyniok, *Compressed Sensing: Theory and Applications*. Cambridge University Press, 2012.

[24] D. L. Donoho, "Compressed sensing," *IEEE Trans. Inf. Theory*, vol. 52, no. 4, pp. 1289–1306, Apr. 2006.

Downloaded From: https://www.spiedigitallibrary.org/conference-proceedings-of-spie on 3/7/2018 Terms of Use: https://www.spiedigitallibrary.org/terms-of-use